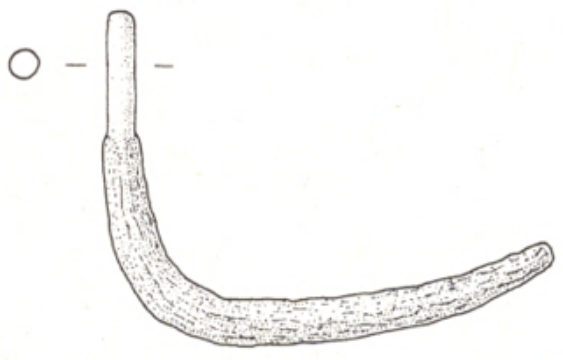
CURVED PIN OR TANG FK 2670.20 – TIN BRONZE – LATE BRONZE AGE – SWITZERLAND

Artefact name Curved pin or tang FK 2670.20

Authors Marianne. Senn (EMPA, Dübendorf, Zurich, Switzerland) & Christian. Degrigny (HE-Arc CR, Neuchâtel, Neuchâtel, Switzerland)

Url /artefacts/515/

The object



Credit HE-Arc CR.

Fig. 1: Curved pin or tang (after Fischer 1997, plate 43),

Description and visual observation

Description of the artefact	Curved pin or tang (Fig. 1). Several samples were taken. Only one is presented here (Fig. 2). The metal is covered with black corrosion products attributed to a burning process mixed with green corrosion products. Dimensions: L = 114mm; Ø = 4.6mm; WT = 16.7g.
Type of artefact	Not defined
Origin	Steinmöri, Neftenbach / Dorf Neftenbach, Zurich, Switzerland
Recovering date	Excavation in 1991?, grave 18
Chronology category	Late Bronze Age
chronology tpq	1400 B.C.
chronology taq	1300 B.C.
Chronology comment	14th Century BC, Bronze Age D
Burial conditions / environment	Soil
Artefact location	Kantonsarchäologie, Dübendorf, Zurich
Owner	Kantonsarchäologie, Dübendorf, Zurich

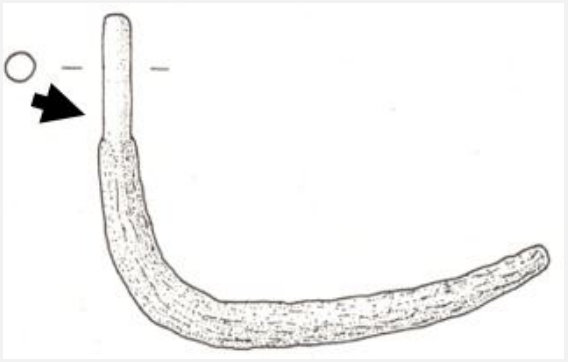
This work is licensed under CC BY-NC-ND 4.0

Inv. number	FK 2670.20
Recorded conservation data	Not conserved

Complementary information

Nothing to report.

Study area(s)



Credit HE-Arc CR.

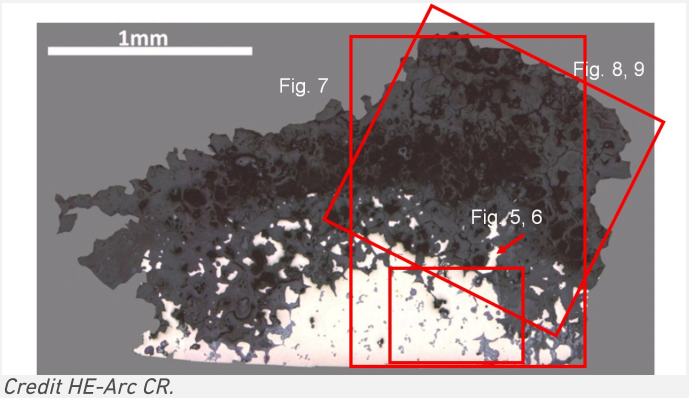
Fig. 2: Location of sampling area,

Binocular observation and representation of the corrosion structure

Stratigraphic representation: none.

MiCorr stratigraphy(ies) – Bi

Sample(s)



Credit HE-Arc CR.

Fig. 3: Micrograph of the cross-section of the sample taken from the curved pin or tang showing the location of Figs. 5 to 9,

Description of sample

The sample (Fig. 3) is a section from the pin (or tang). The metal is covered by a thick corrosion crust (blue layer adhering to the metal, topped by a green layer mixed with black corrosion products - Museum report (1992)). Dimensions: L = 1.8mm; W = 1.2mm.

This work is licensed under CC BY-NC-ND 4.0

Alloy	Tin Bronze
Technology	Secondary recrystallization (produced by burning)
Lab number of sample	MAH 92-5-4-002
Sample location	Musées d'art et d'histoire, Genève, Geneva
Responsible institution	Musées d'art et d'histoire, Genève, Geneva
Date and aim of sampling	1992, examination of metallography examination

Complementary information

Nothing to report.

Analyses and results

Analyses performed:
Metallography (etched with ferric chloride reagent), Vickers hardness testing, EPMA/WDS, SEM/EDS.

Non invasive analysis

Metal

The remaining metal is a tin bronze (Table 1) with copper sulphide inclusions that contain some Fe (Figs. 5 and 6, Table 2). After etching, the tin bronze shows polygonal grains with few twins (Fig. 6). The grain size varies between 70 and 180µm indicating grain growth due to an extended or excessively hot annealing process. The copper sulphide inclusions appear in blue. The average hardness of the metal is HV1 70.

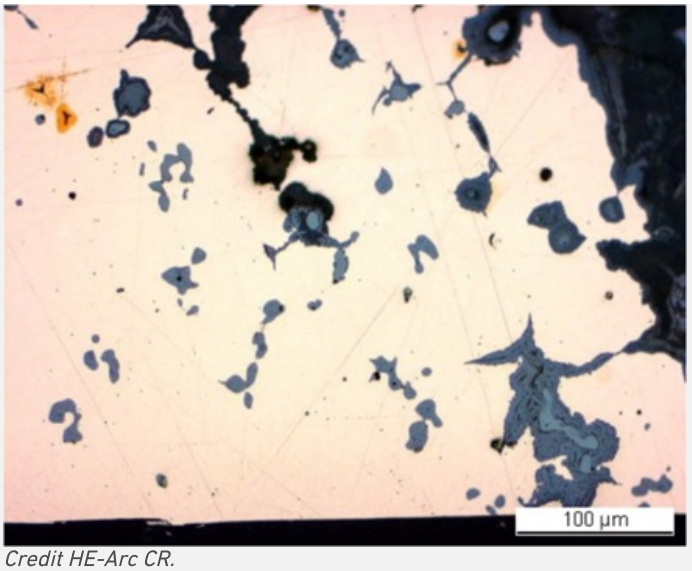
Elements	Cu	Sn	Pb	As	Sb	Fe	Zn	Ag	Au	Co	Bi	Ni	S
mass%	89.94	8.11	0.63	0.41	0.29	0.24	0.13	0.1	0.1	0.04	0.01	<	n. d.

Table 1: Chemical composition of the metal. Method of analysis: EPMA/WDS, Lab Department of Materials, University of Oxford.

Elements	S	Fe	Cu	Total
Dark-blue inclusion	21	2.8	77	102

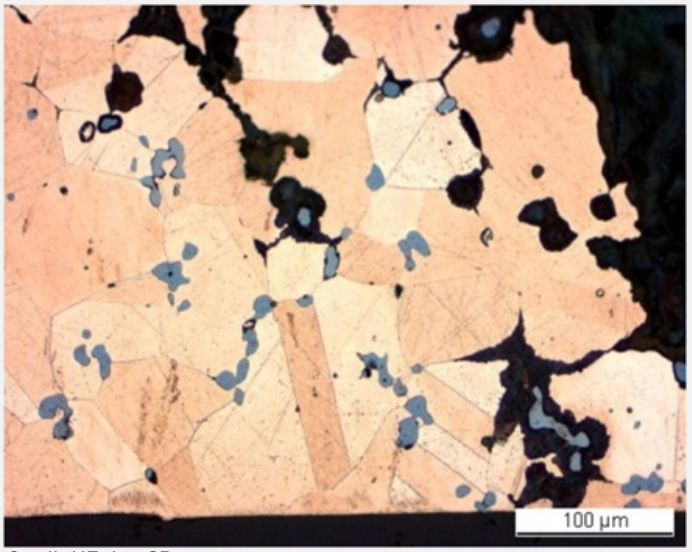
Table 2: Chemical composition (mass %) of the dark-blue inclusions on Fig. 4. Method of analysis: SEM/EDS, Laboratory of Analytical Chemistry, Empa.

This work is licensed under CC BY-NC-ND 4.0



Credit HE-Arc CR.

Fig. 5: Micrograph of the metal sample from Fig. 3 (detail), unetched, bright field. In pink the metal, in light-blue the copper sulphide inclusions and in dark- blue corrosion products,



Credit HE-Arc CR.

Fig. 6: Micrograph of the metal sample from Fig. 3 (same as Fig. 5), etched, bright field. In pink the metal with few twins, in black the resin and the corrosion products, in light-blue the copper sulphide inclusions,

Microstructure	Large polygonal grains with few twins
First metal element	Cu
Other metal elements	Co, Zn, As, Ag, Sn, Sb, Pb, Fe

Complementary information

Nothing to report.

Corrosion layers

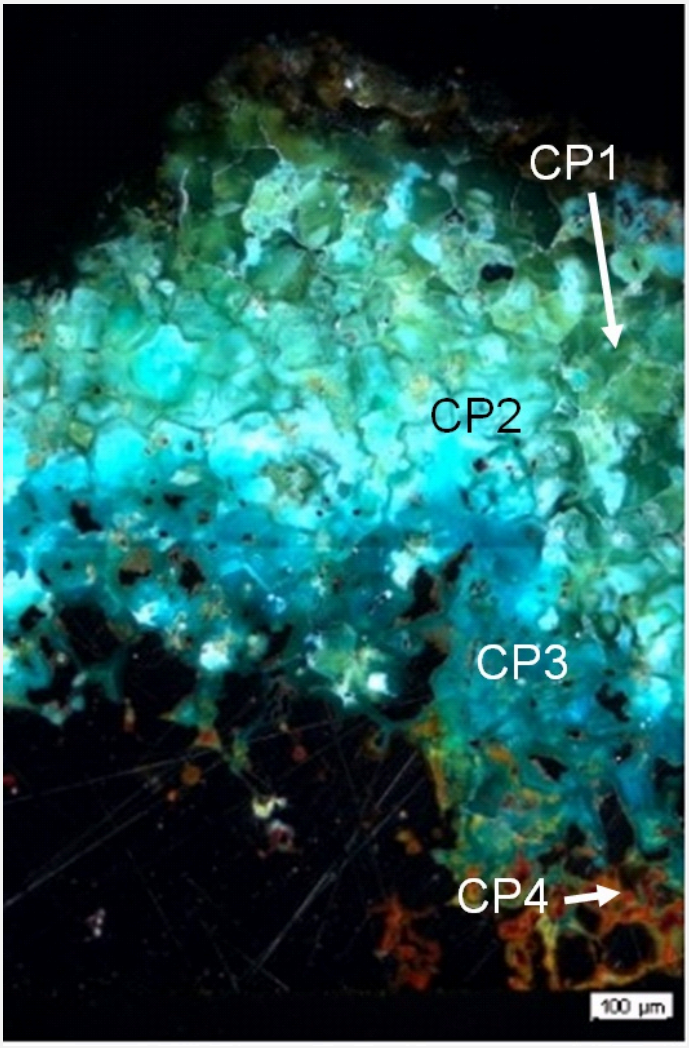
The corrosion crust has an average thickness of 500µm but can in areas be much thicker (Fig. 3). It is divided in two layers. The inner layer is itself divided in two sub-layers: a thin light-grey sub-layer at the interface with the remaining metal surface (CP4, in bright field) which appears red-orange in polarised light (Fig. 7) topped by a medium-grey sub-layer (in bright field) that contains remnant metal (CP3). It turns dark-blue in polarised light (Fig. 7). The outer corrosion layer can also be divided into two sub-layers: a porous sub-layer (CP2) followed by a dark-grey sub-layer in which crystals are outlined by cracks (CP1, in bright field). Under polarized light, the latter turns blue-green while on top it appears olive and brown (Fig. 7). Chemically the corrosion crust is Sn enriched and Cu-depleted (Table 3, Figs. 8 and 9). The maximum of the Sn enrichment occurs on the outer olive and brown sub-layer (CP2). The corrosion layer also contains P, Si, C and O. Inclusions containing Fe or Ag can be found in the corrosion crust (Figs. 8 and 9).

Elements	O	Cu	Sn	Si	P	Fe	Pb	S	Cl	Total

This work is licensed under CC BY-NC-ND 4.0

CP1, outer corrosion layer	27	17	57	1.1	1.9	0.9	1.0	<	<	105
CP3, inner corrosion layer	39	27	26	1.1	2.5	<	<	<	<	97
Remnant metal in CP3	<	88	8.3	<	<	<	<	<	<	97

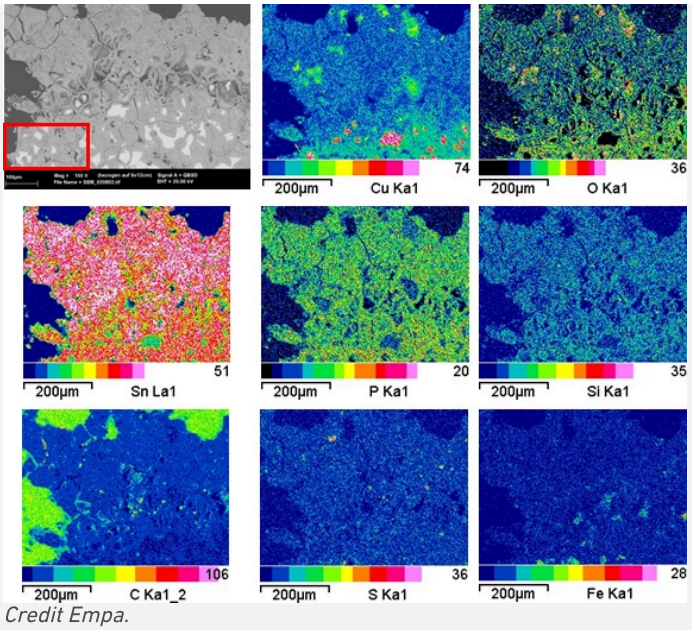
Table 3: Chemical composition (mass %) of the corrosion crust from Fig. 7. Method of analysis: SEM/EDS, Laboratory of Analytical Chemistry, Empa.



Credit HE-Arc CR.

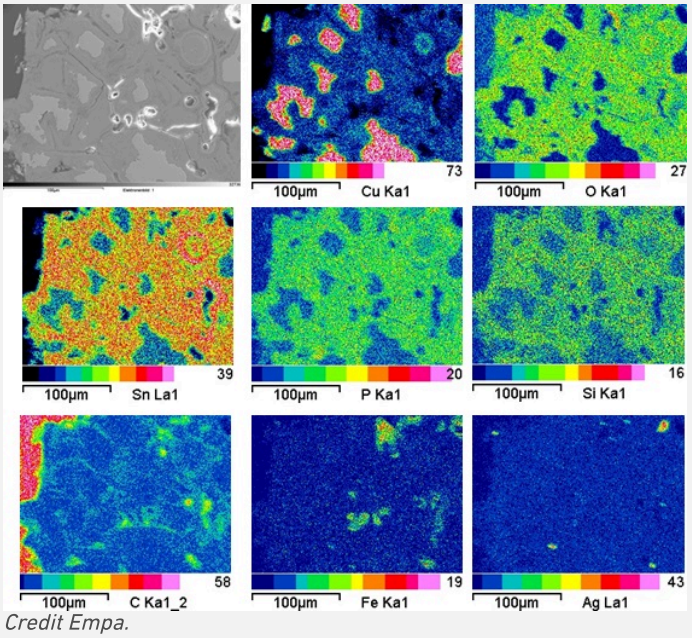
Fig. 7: Micrograph of the metal sample from Fig. 3 (detail) and corresponding to the stratigraphy of Fig. 4, unetched, polarised light. At the metal - corrosion products interface the colour of the corrosion layer is dark-blue, changing to green-blue in the outer part. The top surface of the corrosion crust is olive to brown,

This work is licensed under CC BY-NC-ND 4.0



Credit Empa.

Fig. 8: SEM image, BSE-mode, and elemental chemical distribution of the selected area from Fig. 3 (due to repolishing before SEM/EDX investigation, the SEM image is slightly different from the area indicated in Fig. 3). The rectangle in the SEM image marks the detail mapping of Fig 9. Method of examination: SEM/EDS, Laboratory of Analytical Chemistry, Empa,



Credit Empa.

Fig. 9: SEM image, SE-mode, and elemental chemical distribution of the selected area from Fig. 8. Method of examination: SEM/EDS, Laboratory of Analytical Chemistry, Empa,

Corrosion form	Uniform - intergranular
Corrosion type	Type II (Robbiola)

Complementary information

Nothing to report.

MiCorr stratigraphy(ies) – CS

This work is licensed under CC BY-NC-ND 4.0

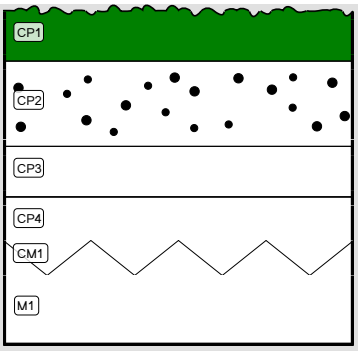


Fig. 4: Stratigraphic representation of the sample taken from the curved pin or tang in cross-section using the MiCorr application. The characteristics of the strata are only accessible by clicking on the drawing that redirects you to the search tool by stratigraphy representation. This representation can be compared to Fig. 7, Credit HE-Arc CR.

Synthesis of the binocular / cross-section examination of the corrosion structure

Corrected stratigraphic representation: none.

Conclusion

The tin bronze was exposed to an extended or excessively hot annealing process. This, combined with the extreme thickness of the corrosion crust and the dark surface, confirms that the object originates from a fire burial context. At the metal - corrosion crust interface some copper oxide (cuprite?) occurs. On top copper carbonates (azurite or malachite?) are mixed with tin oxide (cassiterite/SnO2?). Tin oxide dominates in the brown-black extremely Sn-rich outer layer. The P-enrichment in the whole corrosion layer may be due to an environment rich in organic material (for example bones). The original surface of the metal has been destroyed, presenting a type 2 corrosion layer after Robbiola et al. 1998.

References

References on object and sample

Reference object

1. Fischer, C. (1997) Innovation und Tradition in der Mittel- und Spätbronzezeit. Monographien der Kantonsarchäologie Zürich 28 (Zürich und Egg), 181 and plate 43.

Reference sample

2. Fischer, C. (1997) Innovation und Tradition in der Mittel- und Spätbronzezeit. Monographien der Kantonsarchäologie Zürich 28 (Zürich und Egg), 96.

3. Rapport d'examen 92-5-4 (Schweizer, F. and degli Agosti, M.), Laboratoire Musées d'art et d'histoire, Geneva GE (1992).

References on analytic methods and interpretation

4. Robbiola, L., Blengino, J-M., Fiaud, C. (1998) Morphology and mechanisms of formation of natural patinas on archaeological Cu-Sn alloys, Corrosion Science, 40, 12, 2083-2111.

This work is licensed under CC BY-NC-ND 4.0